AIAA-95-33

DYNAMIC MODELING OF A ROTATING FLEXIBLE BODY

Naveed M. Hussain, Staff Engineer
John F. Kelley, Senior Scientist
Hughes Space and Communications Company
El Segundo, CA 90245

Robert A. Laskin, CSI Task Manager
Jet Propulsion Laboratory
Pasadena, CA 91109

Abstract

This paper presents a practical methodology to analyze the motion of a flexible body that is performing large overall motions. The equations of motion for systems of this type are complex and computationally demanding to solve. This method is practical due its computational tractability and thus the possibility of applying it to real-time simulation. The equations of motion for a flexible body performing arbitrarily large overall motions are derived herein. We investigate an approach that involves computing time-independent modal integrals from finite element model data and couple the rigid body equations and the linear flexible equations retaining only the dominant terms. These terms are chosen according to the degree of modeling accuracy required. A simple example system is formulated and is employed to demonstrate validity of this technique as well as to illustrate theoretical concepts involving floating reference frames made use of in this work.

1. Introduction

When a flexible body is performing large overall motions as well as undergoing small deformations, a method to accurately model the body may be required. An example of this type of system is a flexible spacecraft that is spinning or tumbling. The goal of this work is to provide a methodology of employing a commercial Finite Element Model (FEM) analysis tool such as NASTRAN in conjunction with a rigid-body dynamics analysis tool such as SD/FAST [9] or AUTOSIM [11] to analyze a rotating flexible body. Of course, interface code must be written to include the terms that couple the flexible dynamics and the rigid body dynamics.

This area of research has been extensively studied and a brief historical background is given here. A thorough presentation on the history of floating reference frames is given in Canavin and Likins [3]. Banerjee and Dickens [1] present a very rigourous and complete account on the dynamics of rotating flexible bodies. They validate their results with those shown in Kane et. al [6], however, both these methods introduce computational complexity that may render them impractical for certain applications. General purpose code such as ALLFLEX [3] and DADS [12] have been written to handle systems of this type as well as those that are comprised of articulated flexible bodies, however, once again they require large amounts of computational effort. The main reason why these tools become impractical is because the analyst is not free to choose the dominant terms necessary to solve his/her problem. The motivation in our work is to provide a methodology along with a rigorous analytical basis to make use of existing rigid and flexible body tools to determine the motion of rotating flexible bodies.

The paper is organized as follows. First, an example problem consisting of two rigid bodies with a six-degree-of-freedom elastic coupling is described in detail and a "truth model" is constructed for the purpose of comparison to later approximations. A linear model is then derived for this simple example. Next, the topic of floating reference frames is addresssed and the Tisserand Frame as well as the Linearized Tisserand Frame are discussed. The example system is used to illustrate the properties of these floating reference frames. The next section presents a decoupled methodology. Illustrative examples are provided that show when this method breaks down. Next, the analysis for a lumped element model of a flexible body is carried out providing the equations of motion in complete detail. These equations treat the system as being comprised of lumped rigid bodies with mass and inertia, not simply particles as in [12]. These equations are simplified in the next section resulting in a one-way-coupled methodology. Again, this is illustrated with the example system. Finally, some concluding remarks are given.

2. Example Description

In order to validate the study of tumbling flexible bodies and provide some insight into the

theory, an example was constructed that captures important dynamic coupling effects that are present when motions of the type under consideration are performed. The example system consists of two rigid bodies, A and B, connected together through a six-degree-of-freedom elastic coupling and is shown in Fig. 1. This coupling between the two bodies provides the ability to choose differing spring constants in the three translational degrees of freedom, as well as differing spring constants in the three rotational degrees of freedom. Most importantly, this model exhibits linear behaviour in the region where the relative rotational and translational displacements are small. It was for this reason that this model was chosen over one that employed a single translational spring and a single rotational spring.

The angular velocity of A in the Newtonian reference frame, N, may be written as follows:

$$^N\boldsymbol{\omega}^A = u_1\mathbf{a}_1 + u_2\mathbf{a}_2 + u_3\mathbf{a}_3 \tag{1}$$

where $\mathbf{a}_i$ $(i=1,2,3)$ are unit vectors fixed in A (see Fig. 1). The right superscript of $\boldsymbol{\omega}$ is the body under consideration and the left superscript is the reference frame relative to which the body has an angular velocity. Both of these superscripts are necessary in order to write a meaningful quantity, however, for brevity the left superscript will be dropped when an inertial angular velocity is implied. That is, for the remainder of this report $\boldsymbol{\omega}^A$ is the angular velocity of A in N and similarly, $\mathbf{v}^P$ is the velocity of P in N, where P is a point. We can now write the velocity of A^*, the center of mass of A, as

$$\mathbf{v}^{A^*} = u_4\mathbf{a}_1 + u_5\mathbf{a}_2 + u_6\mathbf{a}_3 \tag{2}$$

The angular velocity of B in A is as follows:

$$^A\boldsymbol{\omega}^B = u_7\mathbf{b}_1 + u_8\mathbf{b}_2 + u_9\mathbf{b}_3 \tag{3}$$

where $\mathbf{b}_i$ $(i=1,2,3)$ are unit vectors fixed in B. Making use of the angular velocity addition theorem, the angular velocity of B in N can be written

$$\boldsymbol{\omega}^B = \boldsymbol{\omega}^A + {}^A\boldsymbol{\omega}^B$$

$$= u_1\mathbf{a}_1 + u_2\mathbf{a}_2 + u_3\mathbf{a}_3 + u_7\mathbf{b}_1 + u_8\mathbf{b}_2 + u_9\mathbf{b}_3 \tag{4}$$

The quantities u_i $(i=1, \ldots, 9)$ are known as *generalized speeds*. The system under consideration possesses twelve generalized speeds. The first six, $u_1, \ldots, u_6$, correspond to the motion of A in the inertial frame N and the last six, $u_7, \ldots, u_{12}$ correspond to the motion of B relative to A. In order to relate these quantities to the *generalized coordinates*, twelve first-order ordinary differential equations known as the *kinematical differential equations* must be specified. These will be presented shortly.

The scheme used to bring B into a desired orientation relative to A is a body-fixed sequence of simple rotations (BODY123). That is, align $\mathbf{b}_i$ with $\mathbf{a}_i$ $(i=1,2,3)$ and subject B to a $\mathbf{b}_1$ rotation of amount q_7, a $\mathbf{b}_2$ rotation of amount q_8, and a $\mathbf{b}_3$ rotation of amount q_9. The three kinematical differential equations relating q_i to u_i $(i=7,8,9)$ are

$$\dot{q}_7 = [u_7\cos(q_9) - u_8\sin(q_9)]/\cos(q_8) \tag{5}$$

$$\dot{q}_8 = u_7\sin(q_9) + u_2\cos(q_9) \tag{6}$$

$$\dot{q}_9 = [-u_7\cos(q_9) + u_8\sin(q_9)]\sin(q_8)/\cos(q_8) + u_9 \tag{7}$$

At each respective rotational "joint" i, there exists a linear rotational spring with spring constant k_i^R $(i=1,2,3)$. In order to include the rotational springs in the equations of motion, we define two massless frames C and D in which the unit vectors $\mathbf{c}_i$ and $\mathbf{d}_i$ $(i=1,2,3)$ are respectively fixed. Thus the torque exerted by A on C, $\mathbf{T}^{A/C}$, can be written

$$\mathbf{T}^{A/C} = -k_1^R q_7 \mathbf{c}_1 \tag{8}$$

where $\mathbf{c}_1 = \mathbf{a}_1$, $\mathbf{c}_2 = \cos(q_7)\,\mathbf{a}_2 + \sin(q_7)\,\mathbf{a}_3$, and $\mathbf{c}_3 = \mathbf{c}_1 \times \mathbf{c}_2$. Similarly, $\mathbf{T}^{C/D}$ can be written

$$\mathbf{T}^{C/D} = -k_2^R q_8 \mathbf{d}_2 \tag{9}$$

where $\mathbf{d}_2 = \mathbf{c}_2$, $\mathbf{d}_3 = \cos(q_8)\,\mathbf{c}_3 + \sin(q_8)\,\mathbf{c}_1$, and $\mathbf{d}_1 = \mathbf{d}_2 \times \mathbf{d}_3$. Finally, $\mathbf{T}^{D/B}$ can be written

$$\mathbf{T}^{D/B} = -k_3^R q_9 \mathbf{b}_3 \tag{10}$$

To add the effect of translational flexibility in each direction, three springs are employed. The first translational spring is attached between A^* and O, a point fixed in C, and has the spring constant k_1^L and natural length L_1. The position vector from A^* to O, $\mathbf{p}^{A^*O}$, is written

$$\mathbf{p}^{A^*O} = q_{10}\mathbf{a}_1 \tag{11}$$

and the force exerted by A^* on O is

$$\mathbf{F}^{A^*/O} = -k_1^L(q_{10} - L_1)\mathbf{a}_1 \tag{12}$$

The second translational spring is attached between O and P, a point fixed in D, and has the spring constant k_2^L and natural length L_2. The position vector from O to P and the force exerted on P by O are

$$\mathbf{p}^{OP} = q_{11}\mathbf{c}_2 \tag{13}$$

$$\mathbf{F}^{O/P} = -k_2^L(q_{11} - L_2)\mathbf{c}_2 \tag{14}$$

Finally, the third translational spring is attached between P and B^* and the corresponding position

and force vectors are

$$\mathbf{p}^{PB^*} = q_{12}\,\mathbf{b}_3 \tag{15}$$

$$\mathbf{F}^{P/B^*} = -k_3^L(q_{12} - L_3)\,\mathbf{b}_3 \tag{16}$$

To complete the kinematics of the system, the position vector, $\mathbf{p}^{A^*B^*}$, from A^* to B^* is written

$$\mathbf{p}^{A^*B^*} = q_{10}\,\mathbf{a}_1 + q_{11}\,\mathbf{c}_2 + q_{12}\,\mathbf{b}_3 \tag{17}$$

and can be expressed in A as

$$\mathbf{p}^{A^*B^*} = [q_{10} + q_{12}\sin(q_8)]\,\mathbf{a}_1 + [q_{11}\cos(q_7) - q_{12}\sin(q_7)\cos(q_8)]\,\mathbf{a}_2 + [q_{11}\sin(q_7) + q_{12}\cos(q_7)\cos(q_8)]\,\mathbf{a}_3 \tag{18}$$

The remaining three generalized speeds, u_i (i=10,11,12) are defined simply as

$$u_i = \dot{q}_i \quad (i=10,11,12) \tag{19}$$

and the velocity of B^* in N is given by

$$\mathbf{v}^{B^*} = \mathbf{v}^{A^*} + \boldsymbol{\omega}^A \times \mathbf{p}^{A^*B^*} + \frac{^A d}{dt}\mathbf{p}^{A^*B^*} \tag{20}$$

where $\frac{^A d}{dt}()$ indicates time-differentiation in the A frame. The generalized coordinates $q_1, \ldots, q_6$ are associated with the location of a point fixed in A and the orientation of A in N. There are many ways to represent this information and the method chosen will govern the form of the kinematical differential equations relating q_i to u_i (i=1, . . . , 6). One method is to let q_i (i=1,2,3) represent the BODY123 angles from N to A [as q_i (i=7,8,9) are the BODY123 angles from A to B], and let q_i (i=4,5,6) be defined as follows:

$$\dot{q}_i = \mathbf{v}^{A^*} \cdot \mathbf{N}_{(i-3)} \quad (i=4,5,6) \tag{21}$$

where $\mathbf{N}_i$ (i=1,2,3) are unit vectors fixed in N.

Only the essential kinematics and geometry have been provided in this report and an automatic equation of motion generator such as SD/FAST or AUTOSIM may now be used to construct the complete equations of motion for this twelve-degree-of-freedom system.

Linear Model

The linear equations of motion for this two-body flexible system may be written as

$$\mathbf{M}\ddot{\mathbf{x}} + \mathbf{G}\dot{\mathbf{x}} + \mathbf{K}\mathbf{x} = \mathbf{F} \tag{22}$$

where $\mathbf{M}$ is a 12×12 mass matrix, $\mathbf{G}$ is a 12×12 damping matrix, $\mathbf{K}$ is a 12×12 stiffness matrix, and $\mathbf{F}$ is a 12×1 force column matrix. The 12×1 column matrix $\mathbf{x}$ is made up of the following states:

$$\mathbf{x} = [x_1^A\ x_2^A\ x_3^A\ \theta_1^A\ \theta_2^A\ \theta_3^A\ x_1^B\ x_2^B\ x_3^B\ \theta_1^B\ \theta_2^B\ \theta_3^B]^T \tag{23}$$

where x_i^A and x_i^B (i=1,2,3) are the respective positions of the center of mass of A and B, and θ_i^A and θ_i^B (i=1,2,3) are the respective orientations of A and B. Since this example contains no damping terms the matrix $\mathbf{G}$ is zero. If the mass of A is m_A, the mass of B is m_B, the inertia matrix of A about A^* is

$$I^{A/A^*} = \begin{bmatrix} I_A & 0 & 0 \\ 0 & J_A & 0 \\ 0 & 0 & K_A \end{bmatrix} \tag{24}$$

and the inertia matrix of B about B^* is

$$I^{B/B^*} = \begin{bmatrix} I_B & 0 & 0 \\ 0 & J_B & 0 \\ 0 & 0 & K_B \end{bmatrix} \tag{25}$$

then the mass matrix is given by

$$\mathbf{M} = \begin{bmatrix} \mathbf{M}_A & 0 \\ 0 & \mathbf{M}_B \end{bmatrix} \tag{26}$$

where

$$\mathbf{M}_A = \begin{bmatrix} m_A & 0 & 0 & 0 & 0 & 0 \\ 0 & m_A & 0 & 0 & 0 & 0 \\ 0 & 0 & m_A & 0 & 0 & 0 \\ 0 & 0 & 0 & I_A & 0 & 0 \\ 0 & 0 & 0 & 0 & J_A & 0 \\ 0 & 0 & 0 & 0 & 0 & K_A \end{bmatrix} \tag{27}$$

and

$$\mathbf{M}_B = \begin{bmatrix} m_B & 0 & 0 & 0 & 0 & 0 \\ 0 & m_B & 0 & 0 & 0 & 0 \\ 0 & 0 & m_B & 0 & 0 & 0 \\ 0 & 0 & 0 & I_B & 0 & 0 \\ 0 & 0 & 0 & 0 & J_B & 0 \\ 0 & 0 & 0 & 0 & 0 & K_B \end{bmatrix} \tag{28}$$

The stiffness matrix is given by

$$\mathbf{K} = \begin{bmatrix} \mathbf{K}_S & -\mathbf{K}_S \\ -\mathbf{K}_S & \mathbf{K}_S \end{bmatrix} \tag{29}$$

where

$$\mathbf{K}_S = \begin{bmatrix} k_1^L & 0 & 0 & 0 & 0 & 0 \\ 0 & k_2^L & 0 & 0 & 0 & 0 \\ 0 & 0 & k_3^L & 0 & 0 & 0 \\ 0 & 0 & 0 & k_1^R & 0 & 0 \\ 0 & 0 & 0 & 0 & k_2^R & 0 \\ 0 & 0 & 0 & 0 & 0 & k_3^R \end{bmatrix} \tag{30}$$

Theoretical concepts introduced in this report will be illustrated using this example system. The full non-linear differential equations of motion will provide a "truth model" to provide a comparison to theories making use of various approximations. The linear set of equations will be employed in several algorithms that attempt to recreate the results of the full equations of motions.

3. The Tisserand Frame

The subject of defining a *floating reference frame* relative to which deformations of an elastic body remain small (in the linear sense) has been an active research topic for over 100 years. An extensive historical overview and background discussion are provided in [3]. The goal of a floating reference frame is to optimally follow the deformable body such that the internal kinetic energy is minimized. When such a frame is employed, the results obtained from a linear vibration analysis have greater validity than those which measure deformations from an inertially fixed frame or one that does not follow the body optimally. This is because the deformations may grow large due to gross motion of the body. In this study, the *Linearized Tisserand Frame* is employed as the floating reference frame of choice since it greatly simplifies the equations of motion (this point will be adressed further in Section 5) and has been found to optimally follow the body [3]. The constraint conditions of this frame and a further discussion are provided below.

Figure 2 shows a general deformable body in an inertial frame. The definitions of each of the symbols shown in Fig. 2 are as follows:

- D — deformable body
- D^* — center of mass of D
- P_i — generic point of D
- dm — differential mass element at P_i
- $\boldsymbol{\rho}_i$ — vector from center of mass to differential mass element
- $\bar{\boldsymbol{\rho}}_i$ — vector from center of mass to undeformed differential mass element
- $\mathbf{u}^{P_i}$ — deformation vector of P_i
- F — floating reference frame
- N — inertial reference frame
- O — point fixed in N
- $\mathbf{R}$ — vector from O to D^*
- $\mathbf{N}_i$ — unit vectors fixed in N
- $\mathbf{f}_i$ — unit vectors fixed in F

We can now write the inertial angular momentum of D about D^* as

$$\mathbf{H}^{D/D^*} = \mathbf{I}^{D/D^*} \cdot \boldsymbol{\omega}^F + \int_D \boldsymbol{\rho}_i \times \frac{^F d}{dt} \boldsymbol{\rho}_i \, dm \tag{31}$$

where $\frac{^F d}{dt}()$ indicates time differentiation in the F frame and $\int_D$ indicates integration over the entire flexible body D. Here the quantity $\mathbf{I}^{D/D^*}$, the inertia of D about D^*, is not a constant but varies with time since D is not a rigid body. If we require that the floating reference frame be defined such that D possess zero internal angular momentum then the following constraint must be imposed

$$\int_D \boldsymbol{\rho}_i \times \frac{^F d}{dt} \boldsymbol{\rho}_i \, dm = 0 \tag{32}$$

Similarly, we can require that D possess zero internal linear momentum which is satisfied if $\boldsymbol{\rho}_i$ is the vector from D^* to a differential mass element and D^* is fixed in F. From the definition of the center of mass of a system we write

$$\int_D \boldsymbol{\rho}_i \, dm = 0 \tag{33}$$

and taking the time derivative in F results in the constraint

$$\int_D \frac{^F d}{dt} \boldsymbol{\rho}_i \, dm = 0 \tag{34}$$

Equations (32) and (34) are the constraint equations that define the *Tisserand Frame*. The Tisserand Frame possesses all the momentum of the system, that is, the deformations that take place relative to this frame do not contribute to either the linear or the angular momentum. The constraints cited above apply to a general system, even when the deformations are large, and solving these equations for the motion of the Tisserand frame is a complicated process and is not practical for complex problems. Instead, we turn to the Buckens frame [3] which is a linearized version of the Tisserand Frame and is frequently called the Linearized Tisserand Frame in the literature. The constraint equations for the Linearized Tisserand Frame are as follows:

$$\int_D \mathbf{u}^{P_i} \, dm = 0 \tag{35}$$

$$\int_D \bar{\boldsymbol{\rho}}_i \times \mathbf{u}^{P_i} \, dm = 0 \tag{36}$$

The reason that the Linearized Tisserand Frame becomes the practical choice is because this frame is identical to that which follows the displacement resulting in zero strain energy, or the rigid-body mode frame (proven in [3]). For semi-definite systems, there exists a rigid-body mode frame that can possess motion which results in zero strain energy.

Thus, if the deformable body is rigidized to form an *equivalent rigid body*, it is this body that can be analyzed with the non-linear differential equations of motion for arbitrarily large translations and rotations. The Linearized Tisserand Frame is fixed in the equivalent-rigid-body frame and Eqs. (35) and (36) are valid. In order to illustrate this concept and provide further insight into the theory, the example problem of the previous section is studied. Three time-simulations are carried out illustrating the following: 1) close agreement between the general and the Linearized Tisserand Frames, 2) small differences between the two frames, and 3) violation of the linear approximation resulting in poor agreement between the two frames.

In order to calculate the motion of the general Tisserand Frame, we turn to the definition, that is, we determine the motion of the frame that possesses all the linear and angular momentum. The example system comprising two rigid bodies attached with an elastic coupling discussed in Section 2 will be called D. To satisfy the linear momentum requirement, we simply monitor the motion of D^*, the center of mass of the system, which has velocity $\mathbf{v}^{D^*}$. In order to satisfy the angular momentum requirement, we calculate the inertial angular velocity of the Tisserand Frame, T, by making use of the following equation:

$$\boldsymbol{\omega}^T = \left[\mathbf{I}^{D/D^*}\right]^{-1} \cdot \mathbf{H}^{D/D^*} \tag{37}$$

where $\mathbf{I}^{D/D^*}$ is the inertia of D about D^*, and $\mathbf{H}^{D/D^*}$ is the inertial angular momentum of D about D^*. The quantity $\mathbf{I}^{D/D^*}$ varies with time since D is not a rigid body and must be calculated at each instant in time along with $\mathbf{H}^{D/D^*}$. The quantity $\boldsymbol{\omega}^T$ does not represent the motion of any physical body, only the motion of the theoretical Tisserand Frame. It may seem to represent the angular velocity of D, but this is a misconception since D is not a rigid body and thus does **not** possess an angular velocity.

To determine the motion of the Linearized Tisserand Frame, the task is simple. *Euler's Equations* of motion must be solved for a rigid body that has identical mass distribution properties as D in the undeformed state. This equivalent rigid body will be called R. The angular velocity of R in inertial space is $\boldsymbol{\omega}^R$ and the velocity of R^*, the center of mass of R, is $\mathbf{v}^{R^*}$. Recall that R^* is coincident with D^* when D is undeformed. In order to compare the motion of the Tisserand Frame to that of the Linearized Tisserand Frame (or equivalent rigid body), we express $\boldsymbol{\omega}^T$, $\mathbf{v}^{D^*}$, $\boldsymbol{\omega}^R$, and $\mathbf{v}^{R^*}$ in the inertial frame to form a common basis for comparison. There is no need to integrate the kinematical differential equations relating these quantities to the generalized coordinates, since the purpose here is solely comparison.

The mass properties of the two bodies comprising D are chosen arbitrarily as

$$m_A = m_B = 0.5 \text{ kg}$$

$$I_A = 0.5 \quad J_A = 0.4 \quad K_A = 0.3 \text{ kg–m}^2$$

$$I_B = 0.5 \quad J_B = 0.4 \quad K_B = 0.3 \text{ kg–m}^2$$

and the spring constants are

$$k_1^L = k_2^L = k_3^L = k_1^R = k_2^R = k_3^R = 1.0 \text{ N/m}$$

with the natural lengths L_1, L_2, L_3 all set to zero. The initial conditions for the first simulation run are as follows:

$$u_i(0) = 0.1 \text{ rad/sec} \quad (i=1,2,3) \tag{38}$$

$$u_i(0) = 0.1 \text{ m/sec} \quad (i=4,5,6) \tag{39}$$

$$u_i(0) = 0.0 \quad (i=7, \ldots, 12) \tag{40}$$

$$q_i(0) = 0.05 \text{ rad} \quad (i=7,8,9) \tag{41}$$

$$q_i(0) = 0.05 \text{ m} \quad (i=10,11,12) \tag{42}$$

These initial conditions correspond to an inital angular and translational motion of A, with B initially at rest relative to A, and the springs connecting B to A initially stretched. The resulting Tisserand Frame angular velocity measure numbers are shown in Fig. 3a. In the following plots the solid line corresponds to the $\mathbf{N}_1$ measure number, the dashed line corresponds to the $\mathbf{N}_2$ measure number, and the dotted line corresponds to the $\mathbf{N}_3$ measure number of the vector being plotted. Figure 3b shows the Linearized Tisserand Frame angular velocity measure numbers and they can be seen to match those in Fig. 3a. This means that the Linearized Tisserand Frame (or equivalent rigid body) is performing the same motion as that of the general Tisserand Frame. That is, even though the motions of A or B do not resemble that of the equivalent rigid body, the Tisserand Frame (which is extracted from the motions of A and B) indeed does. The time-histories of the center of mass velocity measure numbers of D and R are are identical since the center of mass of D will move exactly as the center

of mass of R does and are not shown. The relative angles between A and B are shown in Fig. 3c and can be seen to be in the "linear" range making the Linearized Tisserand Frame an accurate approximation.

The second simulation is run with the initial conditions in Eqs. (38)-(40) and the following:

$$q_i(0) = 0.2 \text{ rad} \quad (i=7,8,9) \tag{43}$$

$$q_i(0) = 0.2 \text{ m} \quad (i=10,11,12) \tag{44}$$

Now the springs connecting A to B are stretched a larger amount and this will result in a more "violent" motion of A and B with greater relative angles between them. Figure 4a shows the time-history of the Tisserand Frame angular velocity measure numbers which have the same qualitative character as those in Fig. 4b of the Linearized Tisserand Frame. The relative angles between A and B are shown in Fig. 4c and have greater magnitudes than those in Fig. 3g thus making the linear approximation worse than the previous case.

The final simulation is run with the initial conditions in Eqs. (38)-(40) and the following:

$$q_i(0) = 0.3 \text{ rad} \quad (i=7,8,9) \tag{45}$$

$$q_i(0) = 0.3 \text{ m} \quad (i=10,11,12) \tag{46}$$

which represent an even greater stretch in the springs connecting A and B than the second simulation. The Tisserand Frame for this case is shown in Fig. 5a and can be seen to considerably differ from the Linearized Tisserand Frame, shown in Fig. 5b. The large relative angles shown in Fig. 5c contribute to the linear approximation breaking down.

This investigation has shown that when the deformations of an elastic system are small (in the linear sense), the **Linearized Tisserand Frame** provides an accurate floating reference frame that is easy to implement. The use of this frame allows the analyst to use conventional linear dynamics tools while being confident that the gross rigid body motion is largely unaffected by the flexible dynamics if the deformations remain small.

4. Decoupled Rigid/Flex Theory

A simple scheme to analyze a flexible body undergoing large rigid body motions is to analyze the linear dynamics as completely decoupled from the rigid body dynamics and vice versa. The complete solution is then obtained by combining the two separate results. This section outlines the methodology of this theory. Certain rules of thumb can be estabilished as to when this theory is applicable. For example, if a flexibile body is performing a simple spin, the lowest natural frequency of the flexible body should be ten times greater than the spin frequency for this theory to hold. These rules of thumb should only be applied to certain classes of problems and cannot be taken as a general rule in analysis. Since the use of this method is so problem specific, no rules of thumb will be developed in this report. Also, this section will introduce some notation that will be employed further in Section 5.

The linear dynamical equations for an $n+6$ degree-of-freedom system free of both internal damping and external forces can be written as

$$\mathbf{M}\ddot{\mathbf{x}} + \mathbf{K}\mathbf{x} = 0 \tag{47}$$

where $\mathbf{M}$ and $\mathbf{K}$ are the $(n+6)\times(n+6)$ mass and stiffness matricies, respectively. When $\mathbf{M}$ and $\mathbf{K}$ are symmetric, we can find an orthonormal (with respect to $\mathbf{M}$ and $\mathbf{K}$) modal matrix $\mathbf{P}$ by solving an eigenvalue problem with $\mathbf{M}$ and $\mathbf{K}$ [7][8]. In terms of the modal coordinates $\mathbf{q}$ obtained from the linear transformation

$$\mathbf{q} = \mathbf{P}\mathbf{x} \tag{48}$$

the linear modal equations of motion become

$$\ddot{\mathbf{q}} + \mathbf{\Lambda}\mathbf{q} = 0 \tag{49}$$

where $\mathbf{\Lambda}$ is defined as

$$\mathbf{\Lambda} = \mathbf{P}^T\mathbf{K}\mathbf{P} \tag{50}$$

and is a diagonal matrix whose elements are equal to the square of the natural frequencies. If we are dealing with a semi-definite system with six rigid-body degrees of freedom (or modes) and the diagonal elements of $\mathbf{\Lambda}$ are in ascending order, the modal equations of motion have the form

$$\ddot{q}_i = 0 \quad (i=1, \ldots, 6) \tag{51}$$

$$\ddot{q}_i + \lambda_i q_i = 0 \quad (i=7, \ldots, n+6) \tag{52}$$

The equations in (51) are the six linear rigid-body modal equations in terms of the modal coordinates q_i $(i=1, \ldots, 6)$. Since these equations become invalid for large rigid body motions, they will not be used. The equations in (52), however, involve the modal coordinates corresponding to the flexible dynamics. These equations are valid when the deformations and body rates remain small. Thus, we replace equations (51) with the non-linear dynamical and kinematical differential equations for a rigid body (*Euler's Equations*) and retain equations (52) to model the flexible dynamics. This is the essence of the decoupled theory presented here.

The n modal coordinates corresponding to the flexible dynamics will be called q_j^f $(j=1, \ldots, n)$.

Let $\mathbf{u}^{P_i}$ be the displacement (or deformation) vector of a point P_i and let $\boldsymbol{\theta}^{B_i}$ be the "rotation vector" of a frame B_i. Note that the concept of a rotation vector such that

$$\boldsymbol{\omega}^{B_i} = \frac{d}{dt}\boldsymbol{\theta}^{B_i} \tag{53}$$

is true, where $\boldsymbol{\omega}^{B_i}$ is the angular velocity of B_i, is only valid in a linear sense and not true for general non-linear kinematics. The deformation and rotation vectors are written in terms of the modal vectors and the modal coordinates as

$$\begin{bmatrix} \mathbf{u}^{P_1} \\ \boldsymbol{\theta}^{B_1} \\ \cdot \\ \cdot \\ \cdot \\ \mathbf{u}^{P_k} \\ \boldsymbol{\theta}^{B_k} \end{bmatrix} = \begin{bmatrix} \boldsymbol{\phi}_1^1 & \boldsymbol{\phi}_2^1 & \cdots & \boldsymbol{\phi}_n^1 \\ \boldsymbol{\phi}'^1_1 & \boldsymbol{\phi}'^1_2 & \cdots & \boldsymbol{\phi}'^1_n \\ \cdot & \cdot & & \cdot \\ \cdot & \cdot & & \cdot \\ \cdot & \cdot & & \cdot \\ \boldsymbol{\phi}_1^k & \boldsymbol{\phi}_2^k & \cdots & \boldsymbol{\phi}_n^k \\ \boldsymbol{\phi}'^k_1 & \boldsymbol{\phi}'^k_2 & \cdots & \boldsymbol{\phi}'^k_n \end{bmatrix} \begin{bmatrix} q_1^f \\ q_2^f \\ \cdot \\ \cdot \\ \cdot \\ q_{n-1}^f \\ q_n^f \end{bmatrix} \tag{54}$$

where k is the number of points and the number of frames in the linear model, $\boldsymbol{\phi}_j^i$ is the j-th modal displacement vector for P_i, and $\boldsymbol{\phi}'^i_j$ is the j-th modal rotation vector for B_i. These modal vectors make up the elements of the modal matrix $\mathbf{P}$.

Alternatively, the displacement and rotation vectors could be written as

$$\mathbf{u}^{P_i} = \sum_{j=1}^{n} \boldsymbol{\phi}_j^i q_j^f \tag{55}$$

and

$$\boldsymbol{\theta}^{B_i} = \sum_{j=1}^{n} \boldsymbol{\phi}'^i_j q_j^f \tag{56}$$

Differentiating these expressions with respect to time in the floating reference frame, F, leads to the following:

$${}^F\mathbf{v}^{P_i} = \sum_{j=1}^{n} \boldsymbol{\phi}_j^i \dot{q}_j^f \tag{57}$$

$${}^F\boldsymbol{\omega}^{B_i} = \sum_{j=1}^{n} \boldsymbol{\phi}'^i_j \dot{q}_j^f \tag{58}$$

where ${}^F\mathbf{v}^{P_i}$ is the velocity of P_i in the F frame and ${}^F\boldsymbol{\omega}^{B_i}$ is the angular velocity of B_i in the F frame.

Recall that the rigid body dynamics are solved using *Euler's Equations* for the equivalent rigid body (or Linearized Tisserand Frame). In order to combine the results of the flexible dynamics with the rigid body dynamics we write $\mathbf{v}^{P_i}$, the velocity of point P_i in inertial space, as

$$\mathbf{v}^{P_i} = \mathbf{v}^{\bar{P}_i} + {}^F\mathbf{v}^{P_i} \tag{59}$$

where $\bar{P}_i$ is a point that is coincident with P_i and fixed in F. The results of the rigid body dynamics analysis consist of $\mathbf{v}^{D^*}$, the velocity of the center of mass of the body, and $\boldsymbol{\omega}^F$, the angular velocity of the floating reference frame. Equation (59) rewritten in terms of these quantities becomes

$$\mathbf{v}^{P_i} = \mathbf{v}^{D^*} + \boldsymbol{\omega}^F \times \bar{\boldsymbol{\rho}}_i + {}^F\mathbf{v}^{P_i} \tag{60}$$

where $\bar{\boldsymbol{\rho}}_i$ is the position vector from D^* to P_i in the underformed state. The angular velocity of B_i in inertial space, $\boldsymbol{\omega}^{B_i}$, is given by

$$\boldsymbol{\omega}^{B_i} = \boldsymbol{\omega}^F + {}^F\boldsymbol{\omega}^{B_i} \tag{61}$$

To solve for the displacements of the points P_i and the rotations of the frames B_i $(i=1, \ldots, k)$, the kinematical differential equations relating $\mathbf{v}^{P_i}$ and $\boldsymbol{\omega}^{B_i}$ to the generalized coordinates must be solved. For example, if the orientation of B_i is to be characterized as a body-fixed sequence of rotations (BODY123), then a set of equations similar to Eqs. (5)-(7) must be integrated. Similarly, if the position of point P_i is to be coordinatized in inertial space, then the following set of equations may be used:

$$\dot{x}_j^{P_i} = \mathbf{v}^{P_i} \cdot \mathbf{N}_j \quad (j=1,2,3) \tag{62}$$

In order to illustrate this method, we turn once again to the example outlined in Section 2. We first choose a set of conditions that result in a close agreement between the use of the full non-linear dynamical differential equations and the use of this decoupling method. Next, a set of conditions is chosen such that the decoupling method results in a poor agreement to the "truth model" showing the weakness of this method. Again, no rules of thumb are mentioned since the analyst must measure many factors when determining an appropriate method.

The mass properties, spring constants, and natural lengths are identical to those in the example of Section 3. The first set of initial conditions are given in Eqs. (38)-(42). Recall that these initial conditions represent an initial angular and translational motion of A with B initially at rest relative to A and a nominal stretch in the springs. Also, A and B move "through" one another since their mass centers are collocated. This condition tends to reduce the amount of coupling between the rigid body motion and the flexible dynamics by minimizing centrifugal forces on the bodies. The decoupled method requires solving *Euler's Equations* for the rigidized system in the undeformed state with identical initial conditions corresponding to it's overall

motion. These rigid-body initial conditions are given by

$$\boldsymbol{\omega}^{F}{}_{(t=0)} = 0.1\,\mathbf{f}_1 + 0.1\,\mathbf{f}_2 + 0.1\,\mathbf{f}_3 \qquad (63)$$

and

$$\mathbf{v}^{D^*}{}_{(t=0)} = 0.1\,\mathbf{f}_1 + 0.1\,\mathbf{f}_2 + 0.1\,\mathbf{f}_3 \qquad (64)$$

The initial conditions of the linear model in Section 3 are written as

$$x_i^A = \theta_i^A = 0 \quad (i=1,2,3) \qquad (65)$$

and

$$x_i^B = 0.05 \text{ m}, \quad \theta_i^B = 0.05 \text{ rad} \quad (i=1,2,3) \qquad (66)$$

Figures 6-8 show the simulation results of the two methods. Figure 6a is the $\mathbf{N}_1$ measure numbers of the angular velocity of A determined from the complete model and Figure 6b is the same quanitity determined from the decoupling method. The $\mathbf{N}_2$ and $\mathbf{N}_3$ measure numbers share the qualitative nature of the $\mathbf{N}_1$ measure number are not shown. Figures 7a and 7b are the results for the angular velocity of B. Figures 8a and 8b show the $\mathbf{N}_1$ measure number of the velocity of A^* resulting from each method. The remaining measure numbers of the velocity of A^* and as well as those of B^* have similar results. As can be seen from these figures, the decoupling method provides results that qualitatively match those of the complete model. The six flexible mode frequencies (in rad/sec) for this example are 4.0, 4.0, 4.0, 4.0, 5.0, and 6.667.

We now illustrate a case where the decoupling method breaks down. The mass and stiffness properties are kept identical to the previous example except now the natural lengths of the srings are taken as

$$L_1 = L_2 = L_3 = 2.0 \text{ m} \qquad (67)$$

The initial conditions are chosen to be the following:

$$u_i(0) = 1.0 \text{ rad/sec} \quad (i=1,2,3) \qquad (68)$$

$$u_i(0) = 1.0 \text{ m/sec} \quad (i=4,5,6) \qquad (69)$$

$$u_i(0) = 0.0 \quad (i=7, \ldots, 12) \qquad (70)$$

$$q_i(0) = 0.2 \text{ rad} \quad (i=7,8,9) \qquad (71)$$

$$q_i(0) = 2.2 \text{ m} \quad (i=10,11,12) \qquad (72)$$

These initial conditions correspond to larger initial rates on the motion of A while B is still initially at rest relative to A, and a greater stretch of the springs. Figure 9a shows the $\mathbf{N}_1$ measure numbers of the angular velocity of A from the complete model and Fig. 9b shows the same quantity resulting from the decoupled method. It can be seen that the decoupled results show no resemblence to those of the complete model. The angular velocity of B as well as the velocities of A^* and B^* result in similarly poor comparisons. The large initial rates along with the separation between A and B result in a larger coupling between the rigid and flexible dynamics than the previous example, and this coupling is not taken into account with this method. The six flexible mode frequencies are identical to the previous example.

In this section we have shown that in some instances, the decoupled method provides results which may be adequate to the analyst. The conditions under which this method may be acceptable are characterized by **slow** (compared to the natural frequencies of the flexible body) rigid body motions along with **small** deformations. However, it has also been illustrated that the method possesses many limitations. For a more accurate modeling of flexible bodies, or for modeling those that are performing "fast" rigid body motions (i.e. large spin rates), it becomes necessary to further investigate the coupling between the rigid body and flexible dynamics. This is the goal of the next section.

5. Coupled Rigid/Flex Analysis

In this section, a single flexible body (or "jello cube") performing large overall motions with small deformations is considered. The problem of multiple interconnected flexible bodies is very complex and the single flexible body problem is studied here to gain insight. In some situations, a system composed of interconnected flexible bodies performing small motions relative to one another may be adequately modeled as a single flexible body and the material in this section would then apply to those cases.

When a Finite Element Model (FEM) is generated with a commercial package, two different formulations may be used. The first is a consistent mass model which assembles the mass and stiffness matricies of differing elements (such as plates, beams, and rods) into global mass and stiffness matricies of the entire structure being analyzed. The second is a lumped mass model which forms a discrete mesh of grid points representing the overall structure with each grid point possessing six degrees of freedom. Each of these grid points is like a rigid body with mass and inertia connected with springs to other rigid bodies to make up the complete FEM. When a grid point is modeled simply as a particle of a given mass, then the rotational degrees of freedom are removed thus preserving the non-singular property of the global mass matrix. In many of the

past formulations of a single flexible body the angular velocity of a frame in the FEM was never considered explicitly. In this approach, we consider the FEM to consist of an equal number of particles and frames each with mass and inertia, respectively. Thus, we explicitly carry the angular velocity of frames throughout the analysis. Also, instead of integrals of modal vectors over the whole body, we deal with summations of modal vectors. This results in an approach that carries over to computerized automation in a clear fashion.

Returning to Fig. 2, we write the velocity of D^* as

$$\mathbf{v}^{D^*} = u_1\mathbf{f}_1 + u_2\mathbf{f}_2 + u_3\mathbf{f}_3 \tag{73}$$

and the angular velocity of the floating reference frame, F, as

$$\boldsymbol{\omega}^F = u_4\mathbf{f}_1 + u_5\mathbf{f}_2 + u_6\mathbf{f}_3 \tag{74}$$

where $u_1, \ldots, u_6$ are generalized speeds. We now define an additional n generalized speeds as $\dot{q}_j$ $(j=1, \ldots, n)$. If one follows the standard convention in [4], these generalized speeds would be defined as

$$u_r = \dot{q}_{r-6} \quad (r=7, \ldots, n+6) \tag{75}$$

however, we will continue with the $\dot{q}_j$ convention for simplicity.

The velocity of the i-th grid point, P_i, is given by

$$\mathbf{v}^{P_i} = \mathbf{v}^{D^*} + \boldsymbol{\omega}^F \times (\bar{\boldsymbol{\rho}}_i + \mathbf{u}^{P_i}) + \frac{{}^F d}{dt}\mathbf{u}^{P_i} \tag{76}$$

where $\mathbf{u}^{P_i}$, D^*, and $\bar{\boldsymbol{\rho}}_i$ are shown in Fig. 2. Making use of Eqn. (55), we can rewrite the above equation as

$$\mathbf{v}^{P_i} = \mathbf{v}^{D^*} + \boldsymbol{\omega}^F \times (\bar{\boldsymbol{\rho}}_i + \sum_{j=1}^{n}\boldsymbol{\phi}_j^i q_j) + \sum_{j=1}^{n}\boldsymbol{\phi}_j^i \dot{q}_j \tag{77}$$

The angular velocity of frame B_i (whose center of mass is P_i) can be written as

$$\boldsymbol{\omega}^{B_i} = \boldsymbol{\omega}^F + \sum_{j=1}^{n}\boldsymbol{\phi}'^i_j \dot{q}_j \tag{78}$$

In order to facilitate the formulation of the equations of motion, the $n+6$ partial velocities of P_i and partial angular velocities of B_i $(i=1, \ldots, k)$ are formed [4]. These are as follows:

$$\mathbf{v}_r^{P_i} = \mathbf{f}_i \quad (r=1,2,3) \tag{79}$$

$$\mathbf{v}_r^{P_i} = \mathbf{f}_{r-3} \times (\bar{\boldsymbol{\rho}}_i + \sum_{j=1}^{n}\boldsymbol{\phi}_j^i q_j) \quad (r=4,5,6) \tag{80}$$

$$\mathbf{v}_r^{P_i} = \boldsymbol{\phi}_{r-6}^i \quad (r=7, \ldots, n+6) \tag{81}$$

$$\boldsymbol{\omega}_r^{B_i} = 0 \quad (r=1,2,3) \tag{82}$$

$$\boldsymbol{\omega}_r^{B_i} = \mathbf{f}_{r-3} \quad (r=4,5,6) \tag{83}$$

$$\boldsymbol{\omega}_r^{B_i} = \boldsymbol{\phi}'^i_{r-6} \quad (r=7, \ldots, n+6) \tag{84}$$

The acceleration of P_i can be expressed as

$$\mathbf{a}^{P_i} = \mathbf{a}_R^{P_i} + \mathbf{a}_{RF}^{P_i} + \mathbf{a}_F^{P_i} \tag{85}$$

where $\mathbf{a}_R^{P_i}$, $\mathbf{a}_{RF}^{P_i}$, and $\mathbf{a}_F^{P_i}$ are given by

$$\mathbf{a}_R^{P_i} = \frac{{}^F d}{dt}\mathbf{v}^{D^*} + \boldsymbol{\omega}^F \times \mathbf{v}^{D^*} + \boldsymbol{\alpha}^F \times \bar{\boldsymbol{\rho}}_i + \boldsymbol{\omega}^F \times (\boldsymbol{\omega}^F \times \bar{\boldsymbol{\rho}}_i) \tag{86}$$

$$\mathbf{a}_{RF}^{P_i} = \boldsymbol{\alpha}^F \times \sum_{j=1}^{n}\boldsymbol{\phi}_j^i q_j + 2\boldsymbol{\omega}^F \times \sum_{j=1}^{n}\boldsymbol{\phi}_j^i \dot{q}_j + \boldsymbol{\omega}^F \times (\boldsymbol{\omega}^F \times \sum_{j=1}^{n}\boldsymbol{\phi}_j^i q_j) \tag{87}$$

$$\mathbf{a}_F^{P_i} = \sum_{j=1}^{n}\boldsymbol{\phi}_j^i \ddot{q}_j \tag{88}$$

The angular acceleration of frame B_i can be written as

$$\boldsymbol{\alpha}^{B_i} = \boldsymbol{\alpha}^F + \sum_{j=1}^{n}\boldsymbol{\phi}'^i_j \ddot{q}_j + \boldsymbol{\omega}^F \times \sum_{j=1}^{n}\boldsymbol{\phi}'^i_j \dot{q}_j \tag{89}$$

where

$$\boldsymbol{\alpha}^F = \frac{{}^F d}{dt}\boldsymbol{\omega}^F \tag{90}$$

Generalized Inertia Forces

In order to form the equations of motion of a system of rigid bodies interconnected with elastic springs, we turn to Kane's equations. This involves computing the generalized inertia forces and the generalized active forces for this $n+6$ degree-of-freedom system of k rigid bodies. The contibution of a rigid body B_i to the generalized inertia force is

$$(F_r^*)_{B_i} = \boldsymbol{\omega}_r^{B_i} \cdot \mathbf{T}_{B_i}^* + \mathbf{v}_r^{P_i} \cdot \mathbf{R}_{P_i}^* \tag{91}$$

with

$$\mathbf{R}_{P_i}^* = -m_i\,\mathbf{a}^{P_i} \tag{92}$$

and

$$\mathbf{T}_{B_i}^* = -\boldsymbol{\alpha}^{B_i} \cdot \mathbf{I}^{B_i} - \boldsymbol{\omega}^{B_i} \times \mathbf{I}^{B_i} \cdot \boldsymbol{\omega}^{B_i} \tag{93}$$

where m_i is the mass of P_i and $\mathbf{I}^{B_i}$ is the inertia dyadic of B_i about P_i. For the generalized speeds u_r $(r=1,2,3)$, the generalized inertia forces are

$$-F_r^* = \sum_{i=1}^{k}\mathbf{f}_r \cdot [m_i(\mathbf{a}_R^{P_i} + \mathbf{a}_{RF}^{P_i} + \mathbf{a}_F^{P_i})] \quad (r=1,2,3) \tag{94}$$

which can be written as

$$-F_r^* = \mathbf{f}_r \cdot \sum_{i=1}^{k} m_i \mathbf{a}_R^{P_i} + \mathbf{f}_r \cdot \sum_{i=1}^{k} m_i \left[\boldsymbol{\alpha}^F \times \sum_{j=1}^{n} \boldsymbol{\phi}_j^i q_j + 2\boldsymbol{\omega}^F \times \sum_{j=1}^{n} \boldsymbol{\phi}_j^i \dot{q}_j + \boldsymbol{\omega}^F \times (\boldsymbol{\omega}^F \times \sum_{j=1}^{n} \boldsymbol{\phi}_j^i q_j) \right] + \mathbf{f}_r \cdot \sum_{i=1}^{k} m_i (\sum_{j=1}^{n} \boldsymbol{\phi}_j^i \ddot{q}_j) \quad (r=1,2,3) \tag{95}$$

Making use of the following vector identities

$$\mathbf{a} \cdot (\mathbf{b} \times \mathbf{c}) = \mathbf{b} \cdot (\mathbf{c} \times \mathbf{a}) \tag{96}$$

$$\mathbf{a} \times (\mathbf{b} \times \mathbf{c}) = (\mathbf{a} \cdot \mathbf{c})\mathbf{b} - (\mathbf{a} \cdot \mathbf{b})\mathbf{c} \tag{97}$$

we can write

$$-F_r^* = \mathbf{f}_r \cdot \sum_{i=1}^{k} m_i \mathbf{a}_R^{P_i} + \sum_{i=1}^{k} m_i \left[\boldsymbol{\alpha}^F \cdot (\sum_{j=1}^{n} \boldsymbol{\phi}_j^i q_j \times \mathbf{f}_r) + 2\boldsymbol{\omega}^F \cdot (\sum_{j=1}^{n} \boldsymbol{\phi}_j^i \dot{q}_j \times \mathbf{f}_r) - |\boldsymbol{\omega}^F|^2 \mathbf{f}_r \cdot \sum_{j=1}^{n} \boldsymbol{\phi}_j^i q_j + \boldsymbol{\omega}^F \cdot \mathbf{f}_r (\sum_{j=1}^{n} \boldsymbol{\phi}_j^i q_j \cdot \boldsymbol{\omega}^F) \right] + \sum_{i=1}^{k} m_i \mathbf{f}_r \cdot (\sum_{j=1}^{n} \boldsymbol{\phi}_j^i \ddot{q}_j) \quad (r=1,2,3) \tag{98}$$

Now employing the properties of free-free modes or the Linearized Tisserand Frame, F, which can be stated as

$$\sum_{i=1}^{k} (\sum_{j=1}^{n} \boldsymbol{\phi}_j^i q_j) m_i = 0 \tag{99}$$

$$\sum_{i=1}^{k} (\bar{\boldsymbol{\rho}}_i \times \sum_{j=1}^{n} \boldsymbol{\phi}_j^i q_j) m_i = 0 \tag{100}$$

$$\sum_{i=1}^{k} \mathbf{I}^{B_i} \cdot (\sum_{j=1}^{n} \boldsymbol{\phi}'^i_j \dot{q}_j) = 0 \tag{101}$$

the generalized inertia forces for u_r $(r=1,2,3)$ are written simply as

$$-F_r^* = \mathbf{f}_r \cdot \sum_{i=1}^{k} m_i \mathbf{a}_R^{P_i} = \mathbf{f}_r \cdot (M\, \mathbf{a}^{D^*}) \quad (r=1,2,3) \tag{102}$$

where $M = \sum_{i=1}^{k} m_i$. These can be seen to be the equations of motion for u_r $(r=1,2,3)$ of the equivalent rigid body.

The generalized inertia forces for u_r $(r=4,5,6)$ are given by

$$-F_r^* = \mathbf{f}_{r-3} \cdot \left[\boldsymbol{\alpha}^F \cdot (\sum_{i=1}^{k} \mathbf{I}^{B_i}) + \boldsymbol{\omega}^F \times (\sum_{i=1}^{k} \mathbf{I}^{B_i}) \cdot \boldsymbol{\omega}^F + \sum_{i=1}^{k} (\bar{\boldsymbol{\rho}}_i \times m_i \mathbf{a}_R^{P_i}) \right] + \mathbf{f}_{r-3} \cdot \sum_{i=1}^{k} \left[(\sum_{j=1}^{n} \boldsymbol{\phi}'^i_j \ddot{q}_j \cdot \mathbf{I}^{B_i}) + (\boldsymbol{\omega}^F \times \sum_{j=1}^{n} \boldsymbol{\phi}'^i_j \dot{q}_j) \cdot \mathbf{I}^{B_i} + \sum_{j=1}^{n} \boldsymbol{\phi}'^i_j \dot{q}_j \times \mathbf{I}^{B_i} \cdot \boldsymbol{\omega}^F + \boldsymbol{\omega}^F \times \mathbf{I}^{B_i} \cdot \sum_{j=1}^{n} \boldsymbol{\phi}'^i_j \dot{q}_j + \sum_{j=1}^{n} \boldsymbol{\phi}'^i_j \dot{q}_j \times \mathbf{I}^{B_i} \cdot \sum_{j=1}^{n} \boldsymbol{\phi}'^i_j \dot{q}_j \right] + \mathbf{f}_{r-3} \cdot \sum_{i=1}^{k} m_i \left[\sum_{j=1}^{n} \boldsymbol{\phi}_j^i q_j \times \mathbf{a}_R^{P_i} + \bar{\boldsymbol{\rho}}_i \times (\boldsymbol{\alpha}^F \times \sum_{j=1}^{n} \boldsymbol{\phi}_j^i q_j) + \sum_{j=1}^{n} \boldsymbol{\phi}_j^i q_j \times (\boldsymbol{\alpha}^F \times \sum_{j=1}^{n} \boldsymbol{\phi}_j^i q_j) + \bar{\boldsymbol{\rho}}_i \times (2\boldsymbol{\omega}^F \times \sum_{j=1}^{n} \boldsymbol{\phi}_j^i \dot{q}_j) + \sum_{j=1}^{n} \boldsymbol{\phi}_j^i q_j \times (2\boldsymbol{\omega}^F \times \sum_{j=1}^{n} \boldsymbol{\phi}_j^i \dot{q}_j) + \bar{\boldsymbol{\rho}}_i \times \left\{ \boldsymbol{\omega}^F \times (\boldsymbol{\omega}^F \times \sum_{j=1}^{n} \boldsymbol{\phi}_j^i q_j) \right\} + \sum_{j=1}^{n} \boldsymbol{\phi}_j^i q_j \times \left\{ \boldsymbol{\omega}^F \times (\boldsymbol{\omega}^F \times \sum_{j=1}^{n} \boldsymbol{\phi}_j^i q_j) \right\} + \bar{\boldsymbol{\rho}}_i \times \sum_{j=1}^{n} \boldsymbol{\phi}_j^i \ddot{q}_j + \sum_{j=1}^{n} \boldsymbol{\phi}_j^i q_j \times \sum_{j=1}^{n} \boldsymbol{\phi}_j^i \ddot{q}_j \right] \quad (r=4,5,6) \tag{103}$$

Due to the properties of the Linearized Tisserand Frame stated in Eqs. (99)-(101), certain terms in the above expression are zero, and the simplified generalized inertia forces may be written as

$$-F_r^* = \mathbf{f}_{r-3} \cdot \left[\boldsymbol{\alpha}^F \cdot (\sum_{i=1}^{k} \mathbf{I}^{B_i}) + \boldsymbol{\omega}^F \times (\sum_{i=1}^{k} \mathbf{I}^{B_i}) \cdot \boldsymbol{\omega}^F + \sum_{i=1}^{k} (\bar{\boldsymbol{\rho}}_i \times m_i \mathbf{a}_R^{P_i} \right] + \mathbf{f}_{r-3} \cdot \sum_{i=1}^{k} \left[(\boldsymbol{\omega}^F \times \sum_{j=1}^{n} \boldsymbol{\phi}'^i_j \dot{q}_j) \cdot \mathbf{I}^{B_i} + \sum_{j=1}^{n} \boldsymbol{\phi}'^i_j \dot{q}_j \times \mathbf{I}^{B_i} \cdot \boldsymbol{\omega}^F \right] + \mathbf{f}_{r-3} \cdot \sum_{i=1}^{k} m_i \left[\sum_{j=1}^{n} \boldsymbol{\phi}_j^i q_j \times \mathbf{a}_R^{P_i} + \bar{\boldsymbol{\rho}}_i \times (\boldsymbol{\alpha}^F \times \sum_{j=1}^{n} \boldsymbol{\phi}_j^i q_j) + \sum_{j=1}^{n} \boldsymbol{\phi}_j^i q_j \times (\boldsymbol{\alpha}^F \times \sum_{j=1}^{n} \boldsymbol{\phi}_j^i q_j) + \bar{\boldsymbol{\rho}}_i \times (2\boldsymbol{\omega}^F \times \sum_{j=1}^{n} \boldsymbol{\phi}_j^i \dot{q}_j) + \sum_{j=1}^{n} \boldsymbol{\phi}_j^i q_j \times (2\boldsymbol{\omega}^F \times \sum_{j=1}^{n} \boldsymbol{\phi}_j^i \dot{q}_j) + \bar{\boldsymbol{\rho}}_i \times \left\{ \boldsymbol{\omega}^F \times (\boldsymbol{\omega}^F \times \sum_{j=1}^{n} \boldsymbol{\phi}_j^i q_j) \right\} + \sum_{j=1}^{n} \boldsymbol{\phi}_j^i q_j \times \left\{ \boldsymbol{\omega}^F \times (\boldsymbol{\omega}^F \times \sum_{j=1}^{n} \boldsymbol{\phi}_j^i q_j) \right\} + \sum_{j=1}^{n} \boldsymbol{\phi}_j^i q_j \times \sum_{j=1}^{n} \boldsymbol{\phi}_j^i \ddot{q}_j \right] \quad (r=4,5,6) \tag{104}$$

It can be seen that the first line of the above expression is simply the equations of motion for u_r $(r=4,5,6)$ of a collection of rigid bodies making up a total rigid body. That is, the first line corresponds to the equivalent rigid body of the system.

The remaining generalized inertia forces are those corresponding to u_r $(r=7, \ldots, n+6)$. These

may be written as follows:

$$-F_r^* = \sum_{i=1}^{k} \phi'^{i}_{r-6} \cdot \left[\alpha^F \cdot \mathbf{I}^{B_i} + \sum_{j=1}^{n} \phi'^{i}_{j} \ddot{q}_j \cdot \mathbf{I}^{B_i} + \omega^F \times \mathbf{I}^{B_i} \cdot \omega^F \right.$$

$$+ (\omega^F \times \sum_{j=1}^{n} \phi'^{i}_{j} \dot{q}_j) \cdot \mathbf{I}^{B_i} + \omega^F \times \mathbf{I}^{B_i} \cdot \sum_{j=1}^{n} \phi'^{i}_{j} \dot{q}_j$$

$$\left. + \sum_{j=1}^{n} \phi'^{i}_{j} \dot{q}_j \times \mathbf{I}^{B_i} \cdot \omega^F + \sum_{j=1}^{n} \phi'^{i}_{j} \dot{q}_j \times \mathbf{I}^{B_i} \cdot \sum_{j=1}^{n} \phi'^{i}_{j} \dot{q}_j \right]$$

$$+ \sum_{i=1}^{k} m_i \phi^{i}_{r-6} \cdot \left[\frac{d}{dt} \mathbf{v}^{D^*} + \omega^F \times \mathbf{v}^{D^*} + \alpha^F \times \bar{\rho}_i \right.$$

$$+ \omega^F \times (\omega^F \times \bar{\rho}_i) + \alpha^F \times \sum_{j=1}^{n} \phi^{i}_{j} q_j$$

$$+ 2\omega^F \times \sum_{j=1}^{n} \phi^{i}_{j} \dot{q}_j + \omega^F \times (\omega^F \times \sum_{j=1}^{n} \phi^{i}_{j} q_j)$$

$$\left. + \sum_{j=1}^{n} \phi^{i}_{j} \ddot{q}_j \right] \quad (r=7, \ldots, n+6) \qquad (105)$$

Employing the properties of the Linearized Tisserand Frame, the mass normalization and orthogonality of the modal vectors, and the vector identies in Eqs. (96)-(97), the above equations may be written as

$$-F_r^* = \ddot{q}_{r-6} + \omega^F \cdot \left\{ \sum_{i=1}^{k} \phi^{i}_{r-6} \bar{\rho}_i m_i \right\} \cdot \omega^F$$

$$- |\omega^F|^2 \left\{ \sum_{i=1}^{k} \phi^{i}_{r-6} \cdot \bar{\rho}_i m_i \right\}$$

$$+ \sum_{i=1}^{k} \left[\phi'^{i}_{r-6} \cdot \left\{ (\omega^F \times \sum_{j=1}^{n} \phi'^{i}_{j} \dot{q}_j) \cdot \mathbf{I}^{B_i} \right\} \right.$$

$$\left. + \phi'^{i}_{r-6} \cdot \left\{ \sum_{j=1}^{n} \phi'^{i}_{j} \dot{q}_j \times \mathbf{I}^{B_i} \cdot \omega^F \right\} \right]$$

$$+ \sum_{i=1}^{k} m_i \left[\alpha^F \cdot (\sum_{j=1}^{n} \phi^{i}_{j} q_j \times \phi^{i}_{r-6}) + 2\omega^F \cdot (\sum_{j=1}^{n} \phi^{i}_{j} \dot{q}_j \times \phi^{i}_{r-6}) \right]$$

$$- |\omega^F|^2 q_{r-6} + \omega^F \cdot \left\{ \sum_{i=1}^{k} \phi^{i}_{r-6} (\sum_{j=1}^{n} \phi^{i}_{j} q_j) m_i \right\} \cdot \omega^F$$

$$(r=7, \ldots, n+6) \qquad (106)$$

The terms in curly braces on the first two lines of the above expression depend solely on time-invariant quantities and may be computed ahead of time. These terms will be referred to as *modal integrals.*

Referring to the first term in the second-to-last line of the above expression, the minus sign will cause a "dynamic softening" effect as the magnitude of ω^F increases. This effect should be a "dynamic stiffening" and the *premature linearization* process of the FEM analysis produces this anomaly as pointed out in [10].

Generalized Active Forces

In order to complete the formulation of the equations of motion, the $n+6$ generalized active forces must be formed. The contribution of a generic rigid body, B_i, to the generalized active forces is given by

$$(F_r)_{B_i} = \omega_r^{B_i} \cdot \mathbf{T}^{B_i} + \mathbf{v}_r^{P_i} \cdot \mathbf{R}^{P_i} \qquad (107)$$

where $\mathbf{T}^{B_i}$ is the torque of the couple acting on B_i and $\mathbf{R}^{P_i}$ is the resultant of the contact and/or distance forces whose line of action passes through P_i [4].

The generalized active forces corresponding to u_r $(r=1,2,3)$ may be written as

$$F_r = \sum_{i=1}^{k} \mathbf{f}_r \cdot \mathbf{R}^{P_i} \quad (r=1,2,3) \qquad (108)$$

where $\mathbf{R}^{P_i}$ are the forces acting through P_i. The generalized active forces corresponding to u_r $(r=4,5,6)$ are given by

$$F_r = \sum_{i=1}^{k} \mathbf{f}_{r-3} \cdot \mathbf{T}^{B_i} + \sum_{i=1}^{k} \left\{ \mathbf{f}_{r-3} \times (\bar{\rho}_i + \sum_{j=1}^{n} \phi^{i}_{j} q_j) \right\} \cdot \mathbf{R}^{P_i}$$

$$(r=4,5,6) \qquad (109)$$

and making use of the vector identies in Eqs. (96)-(97) we can write

$$F_r = \sum_{i=1}^{k} \mathbf{f}_{r-3} \cdot \mathbf{T}^{B_i} + \sum_{i=1}^{k} \mathbf{f}_{r-3} \cdot (\bar{\rho}_i \times \mathbf{R}^{P_i})$$

$$+ \sum_{i=1}^{k} \mathbf{f}_{r-3} \cdot (\sum_{j=1}^{n} \phi^{i}_{j} q_j \times \mathbf{R}^{P_i}) \quad (r=4,5,6) \qquad (110)$$

For the generalized active forces corresponding to u_r $(r=7, \ldots, n+6)$, the following holds:

$$F_r = \sum_{i=1}^{k} (\phi'^{i}_{r-6} \cdot \mathbf{T}^{B_i}) + \sum_{i=1}^{k} (\phi^{i}_{r-6} \cdot \mathbf{R}^{P_i}) - \omega_{r-6}^2 q_{r-6}$$

$$- 2\zeta_{r-6} \omega_{r-6} \dot{q}_{r-6} \quad (r=7, \ldots, n+6) \qquad (111)$$

assuming modal stiffness and damping.

Equations of Motion

Now, the equations of motion of the entire system may be assembled by making use of *Kane's Equations of Motion* [4] given by

$$F_r + F_r^* = 0 \quad (r=1, \ldots, n+6) \qquad (112)$$

Retaining all of the terms given in this analysis would be extremeley tedious and impractical when presented a realistic problem. A rationale must be made on how to simplify the problem by neglecting certain terms. A simplified procedure that is based on such an idea is presented in the next section.

6. One-Way Coupling Methodology

In order to improve the decoupled methodology and yet still have a technique that is computationally practical, a one-way coupled technique is introduced herein. The equations of motion derived in the previous section are simplified to the following:

$$\mathbf{f}_r \cdot M\mathbf{a}^{D^*} = \sum_{i=1}^{k} \mathbf{f}_r \cdot \mathbf{R}^{P_i} \quad (r=1,2,3) \qquad (113)$$

$$\mathbf{f}_{r-3} \cdot \left[\boldsymbol{\alpha}^F \cdot (\sum_{i=1}^{k} \mathbf{I}^{B_i}) + \boldsymbol{\omega}^F \times (\sum_{i=1}^{k} \mathbf{I}^{B_i}) \cdot \boldsymbol{\omega}^F + \sum_{i=1}^{k} (\bar{\boldsymbol{\rho}}_i \times m_i \mathbf{a}_R^{P_i}) \right]$$

$$= \sum_{i=1}^{k} \mathbf{f}_{r-3} \cdot \mathbf{T}^{B_i} + \sum_{i=1}^{k} \mathbf{f}_{r-3} \cdot (\bar{\boldsymbol{\rho}}_i \times \mathbf{R}^{P_i}) \quad (r=4,5,6) \qquad (114)$$

$$\ddot{q}_{r-6} + 2\zeta_{r-6}\omega_{r-6}\dot{q}_{r-6} + \omega_{r-6}^2 q_{r-6}$$

$$+ \boldsymbol{\omega}^F \cdot \left\{ \sum_{i=1}^{k} \boldsymbol{\phi}_{r-6}^i \bar{\boldsymbol{\rho}}_i m_i \right\} \cdot \boldsymbol{\omega}^F - |\boldsymbol{\omega}^F|^2 \left\{ \sum_{i=1}^{k} \boldsymbol{\phi}_{r-6}^i \cdot \bar{\boldsymbol{\rho}}_i m_i \right\}$$

$$= \sum_{i=1}^{k} (\boldsymbol{\phi}'^i_{r-6} \cdot \mathbf{T}^{B_i}) + \sum_{i=1}^{k} (\boldsymbol{\phi}_{r-6}^i \cdot \mathbf{R}^{P_i})$$

$$(r=7, \ldots, n+6) \qquad (115)$$

Now we can make some very interesting observations. Equations (113) and (114) are the equations of motion of the equivalent rigid body of the system and **do not** depend on any modal coordinates. That is, the rigid body equations corresponding to u_r $(r=1, \ldots, 6)$ are completely decoupled from the modal equations. However, the modal differential equations in (115) do depend on the rigid body equations and are thus coupled. This means that the rigid body dynamics may be computed **independantly** of the flexible dynamics and the results of this can then be used to apply the appropriate "field forces" that result from the centrifugal acceleration term. The modal integrals (in curly braces) must be computed from the model data at the outset of the computation and need not be repeated. One can notice that the two coupling terms present in (115) are only dependent on translational modal vectors. No rotational coupling is present in these equations and this is a weakness of the method. However, in a practical industry FEM analysis, most of the lumped elements have zero inertia and are simply modeled as particles or they have very small inertia compared to the mass.

Example

Once again, we return to the example of Section 2 in this case to illustrate the one-way coupling methodology. The geometric and mass properties of the example system as well as the initial conditions of motion are chosen such that the advantages as well as the disadvantages of this theory are made apparent. The mass properties are

$$m_A = 10.0 \text{ kg} \quad m_B = 0.3 \text{ kg}$$

$$I_A = 5 \quad J_A = 4 \quad K_A = 3 \text{ kg–m}^2$$

$$I_B = 0.05 \quad J_B = 0.04 \quad K_B = 0.03 \text{ kg–m}^2$$

and the spring constants are

$$k_1^L = k_2^L = k_3^L = k_1^R = k_2^R = k_3^R = 1.0 \text{ N/m}$$

with the natural lengths defined as

$$L_1 = L_2 = L_3 = 2.0 \text{ m}$$

The initial conditions for the simulation are as follows:

$$u_1(0) = 0.1 \text{ rad/sec} \qquad (116)$$

$$u_i(0) = 0.0 \text{ m/sec} \quad (i=4, \ldots, 12) \qquad (117)$$

$$q_i(0) = 0.0 \text{ rad} \quad (i=7,8,9) \qquad (118)$$

$$q_i(0) = 2.0 \text{ m} \quad (i=10,11,12) \qquad (119)$$

which represent an initial angular velocity of A with B initially at rest relative to A and all translational and rotational springs initially at their respective natural lengths.

Figures 10a,b and 11a,b show the results of the non-linear simulation of the example system. It can be seen that flexible motion is induced solely from the overall motion due to dynamic "field forces" that exist. Since the initial conditions on the springs dictate that they are all at their natural lengths initially, the results of the decoupled simulations shown in Figs. 12a,b and 13a,b represent only the motion of the equivalent rigid body (or Linearized Tisserand Frame). These can be seen to capture the overall motion of the two bodies, however, do not include any of the flexible effects. The one-way-coupling method was employed to generate the results shown in Figs. 14a,b and 15a,b. Figures 14a,b shows the angular rate time-histories, and are identical to those in Figs. 12a,b. This fact shows a weakness in the one-way-coupling method, that is, no rotary inertia effects are taken into account. This was mentioned earlier in the report. However, after examining Figs. 15a,b and comparing them to Figs. 13a,b, one can see that the translational motion was affected by the one-way-coupling and provides a

better match to the non-linear simulation shown in Figs. 11a,b. As mentioned earlier, most industry FEM analyses do not include excessive lumped inertia elements so this method will capture many of the effects of a tumbling rigid body.

An Extension to the One-Way Coupling Method

If a higher degree of fidelity is required in an analysis of this sort , more of the terms given in the complete equations of motion should be retained. Another term that could be important is the coriolis acceleration term in Eq. (104) (the last term on the fourth line). Making use of the vector identities in Eqs. (96)-(97), the term under consideration may be written as

$$m_i \bar{\rho}_i \times (2\omega^F \times \sum_{j=1}^{n} \phi_j^i \dot{q}_j) = 2\sum_{j=1}^{n} \dot{q}_j \left[\omega^F \left\{ \sum_{i=1}^{k} \phi_{r-6}^i \cdot \bar{\rho}_i m_i \right\} - \left\{ \sum_{i=1}^{k} \phi_{r-6}^i \bar{\rho}_i m_i \right\} \cdot \omega^F \right] \quad (120)$$

The terms in curly braces can be seen to be the time-independent *modal integrals* mentioned earlier. With the inclusion of the above term, the analysis is further complicated in that the rigid equations may no longer be solved independently. Instead, a coupled integration algorithm must be used. No example has been done here showing the benefits of this extension, however, this is a prime candidate for future work.

7. Conclusions

This paper provides the theoretical results of a study on the dynamics of flexible bodies performing large rigid body motion. An example that captures the main effects of such motion has been defined and used throughout the report to illustrate and provide insight into the theoretical concepts. The coupled dynamical differential equations in vector form of a flexible body have been derived and include the terms resulting from rotary inertia effects. These equations may be used to verify simplifications that may be made in an analysis by calculating representative magnitudes of all the terms. A practical one-way-coupling methodology has been shown and illustrated showing both its strengths and weaknesses.

References

[1] Banerjee, A. K. and Dickens, J. M., "Dynamics of an Arbitrary Flexible Body in Large Rotation and Translation," Journal of Guidance, Control and Dynamics, Vol. 13, No. 2, March 1990.

[2] Canavin, J.R. and Likins, P.W., "Floating Reference Frames for Flexible Spacecraft," *Journal of Spacecraft and Rockets*, Vol. 14, No. 12, December, 1977, pp. 724-732.

[3] Ho, J. Y. L. and Herber, D. R., "Development of Dynamics and Control Simulation of Large Flexible Space Systems," Journal of Guidance, Control and Dynamics, Vol. 8, No. 3, May, 1985.

[4] Kane, T. R. and Levinson, D. A., *Dynamics: Theory and Applications*, McGraw-Hill, New York, 1985.

[5] Kane, T.R., Likins, P.W., and Levinson, D.A., *Spacecraft Dynamics*, McGraw-Hill, New York, 1983.

[6] Kane, T. R. and Ryan, R. R., "Dynamics of a Cantilever Beam Attached to a Moving Base," Journal of Guidance, Control and Dynamics, Vol. 10, No. 2, March 1987.

[7] Kelley, John F. *Linear Dynamics Modeling, A Set of Lecture Notes*, Hughes Aircraft Company, 1991, Draft.

[8] Meirovitch, Leonard, *Elements of Vibration Analysis*, McGraw-Hill, New York, 1986.

[9] Rosenthal, D. E. and Sherman, M. A., "High Performance Multibody Simulations via Symbolic Equation Manipulation and Kane's Method," The Journal of the Astronautical Sciences, Vol. 34, No. 3, July-September, 1986.

[10] Ryan, R. R., "Flexibility Modeling Methods in Multibody Dynamics," AAS/AIAA Astrodynamics Specialist Conference, Paper No. AAS 87-431, Kalispell, Montana, Aug. 10-14, 1987.

[11] Sayers, M. W., "Symbolic Computer Methods to Automatically Formulate Vehicle Simulation Codes." Ph.D. dissertation, The University of Michigan, February 1990.

[12] Yoo, Wan S. and Haug, E. J., "Dynamics of Articulated Structures. Part I. Theory," Journal of Structural Mechanics, Vol. 14, No. 1, 1986.

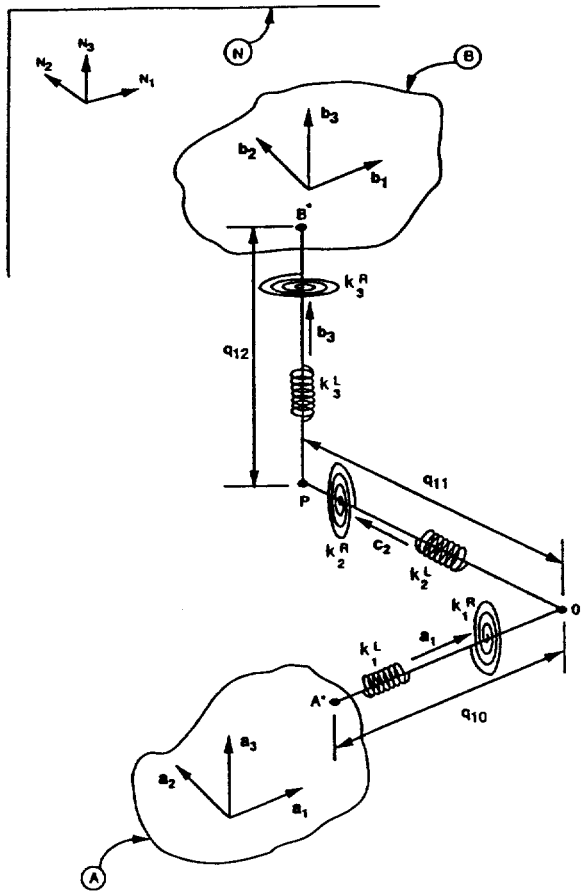

Figure 1: Example Flexible System

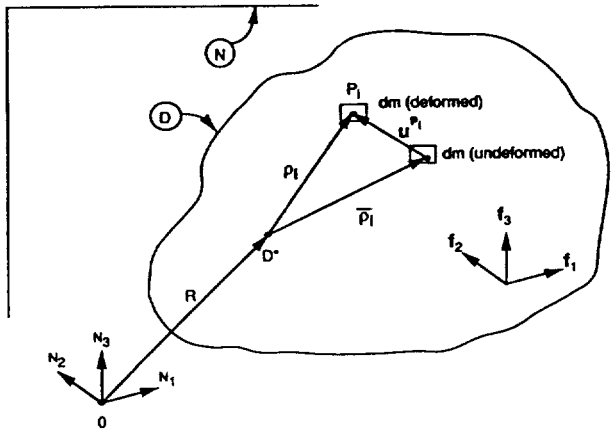

Figure 2: Deformable Body

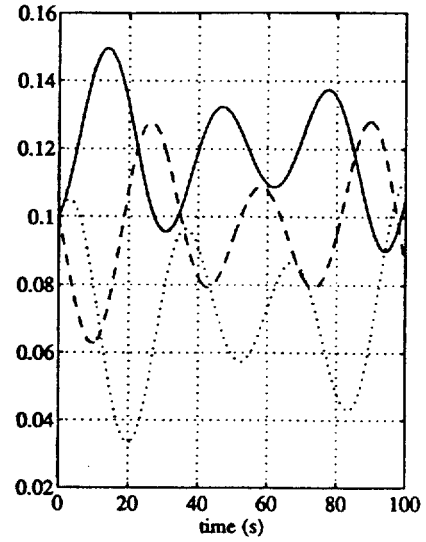

Figure 3a: Tisserand Frame Ang. Rates [rad/s] (case 1)

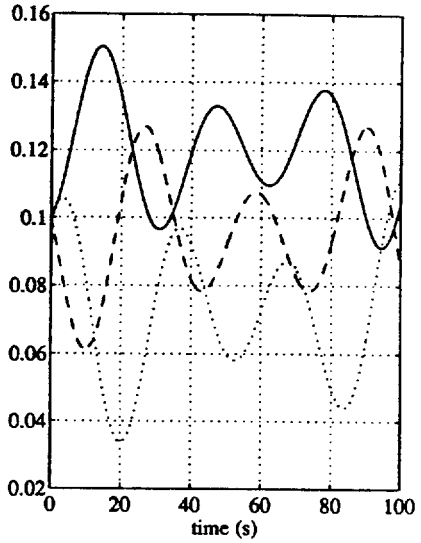

Figure 3b: Linearized Tisserand Ang. Rates [rad/s] (case 1)

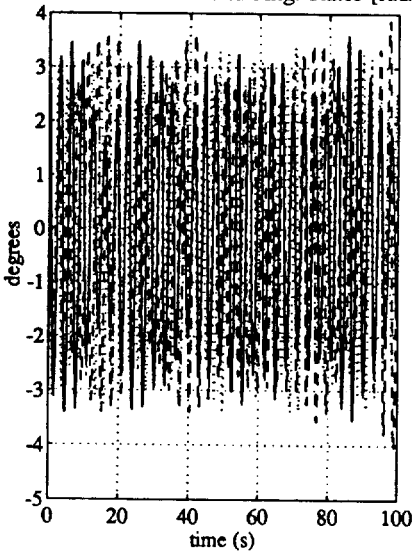

Figure 3c: Relative Angles (case 1)

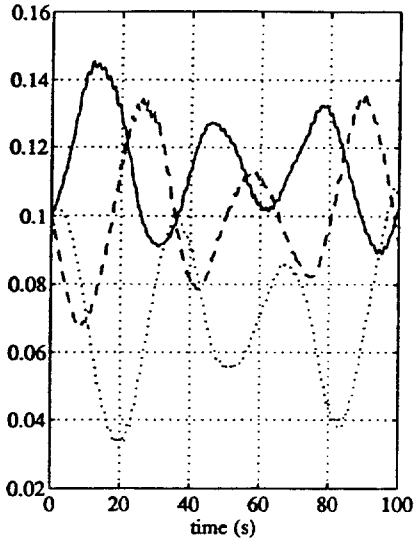

Figure 4a: Tisserand Frame Ang. Rates [rad/s] (case 2)

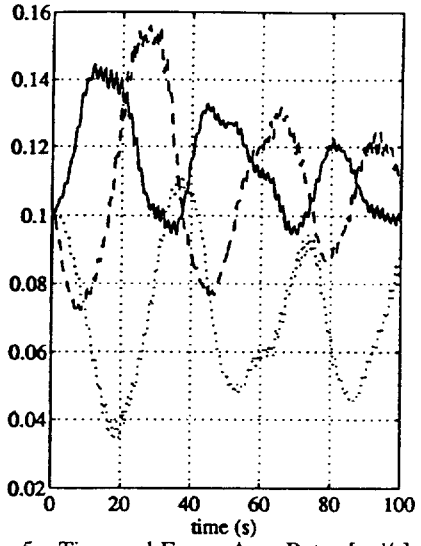

Figure 5a: Tisserand Frame Ang. Rates [rad/s] (case 3)

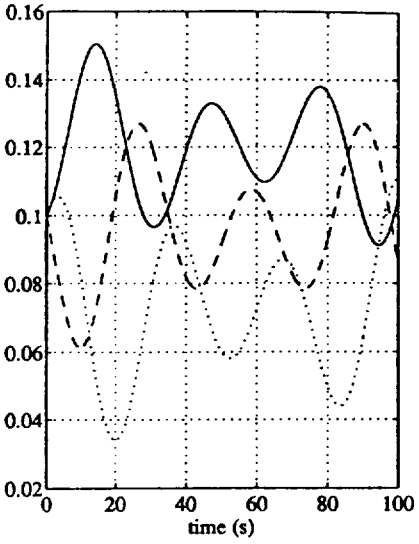

Figure 4b: Linearized Tisserand Frame Ang. Rates [rad/s] (case 2)

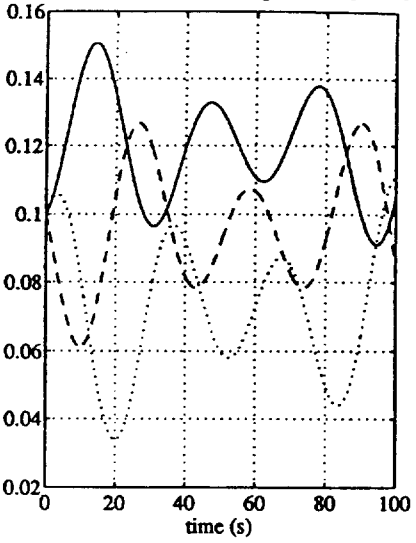

Figure 5b: Linearized Tisserand Frame Ang. Rates [rad/s] (case 3)

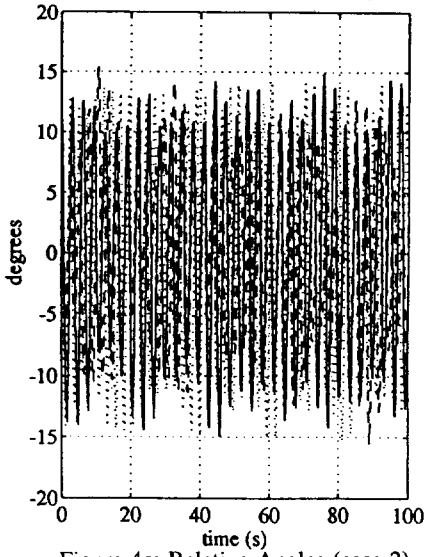

Figure 4c: Relative Angles (case 2)

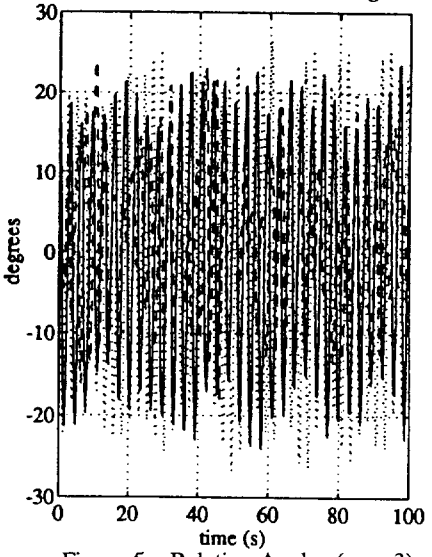

Figure 5c: Relative Angles (case 3)

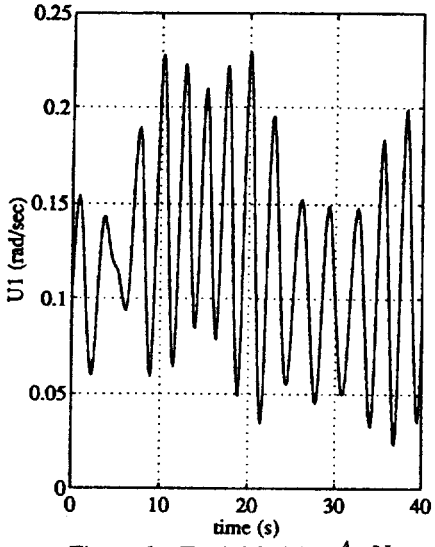

Figure 6a: Truth Model: $\omega^A \cdot \mathbf{N}_1$

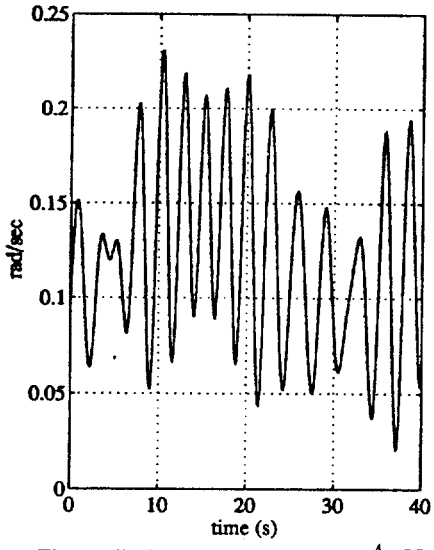

Figure 6b: Decoupled Method: $\omega^A \cdot \mathbf{N}_1$

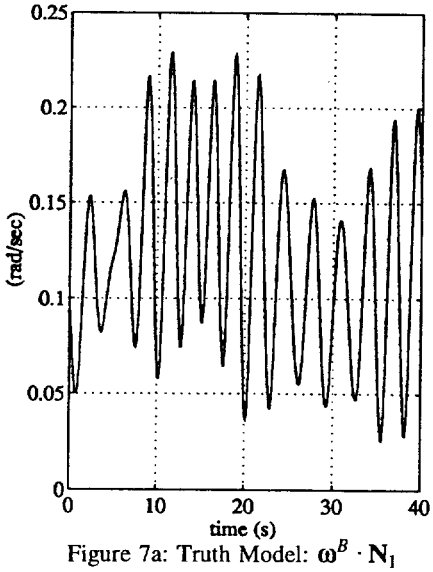

Figure 7a: Truth Model: $\omega^B \cdot \mathbf{N}_1$

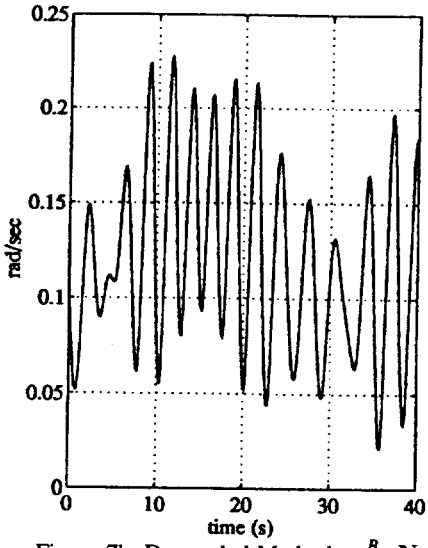

Figure 7b: Decoupled Method: $\omega^B \cdot \mathbf{N}_1$

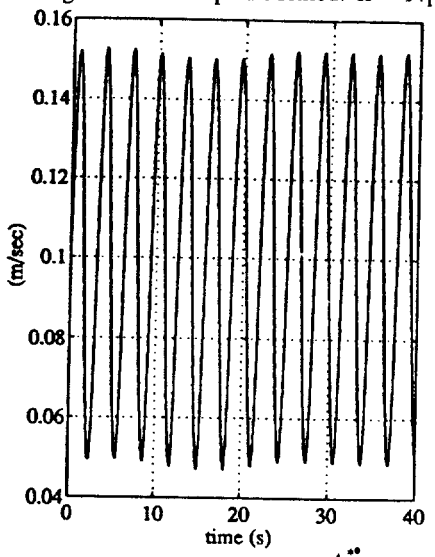

Figure 8a: Truth Model: $\mathbf{v}^{A^{**}} \cdot \mathbf{N}_1$

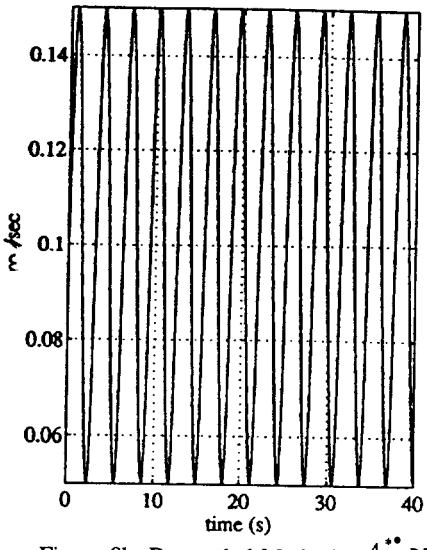

Figure 8b: Decoupled Method: $\mathbf{v}^{A^{**}} \cdot \mathbf{N}_1$

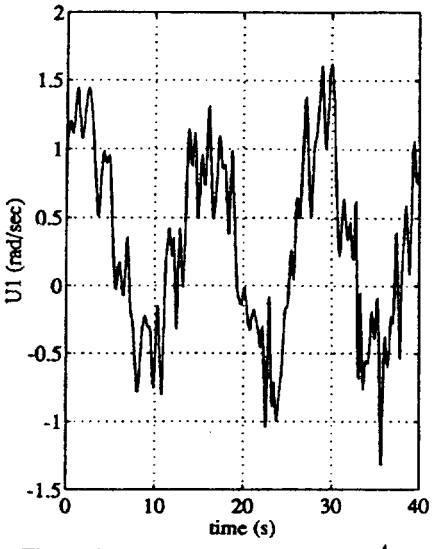

Figure 9a: Truth Model (case 2): $\omega^A \cdot \mathbf{N}_1$

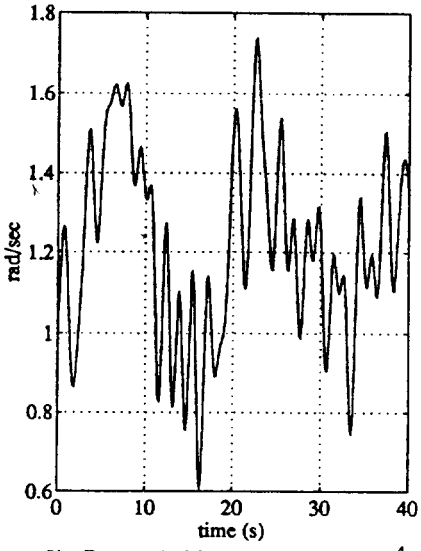

Figure 9b: Decoupled Method (case 2): $\omega^A \cdot \mathbf{N}_1$

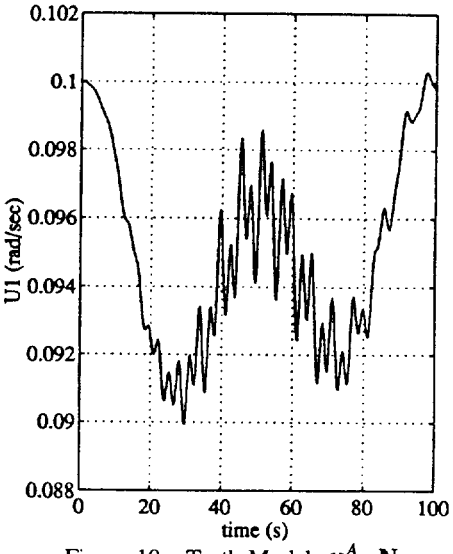

Figure 10a: Truth Model: $\omega^A \cdot \mathbf{N}_1$

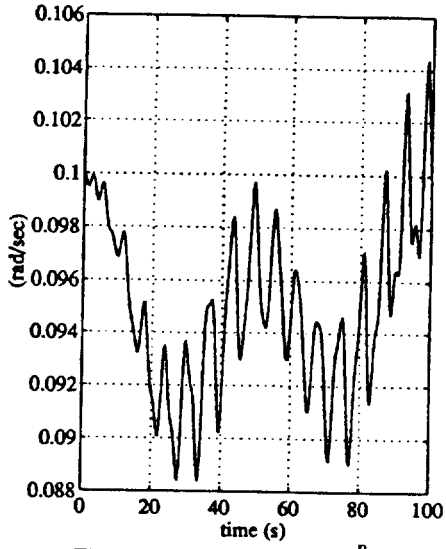

Figure 10b: Truth Model: $\omega^B \cdot \mathbf{N}_1$

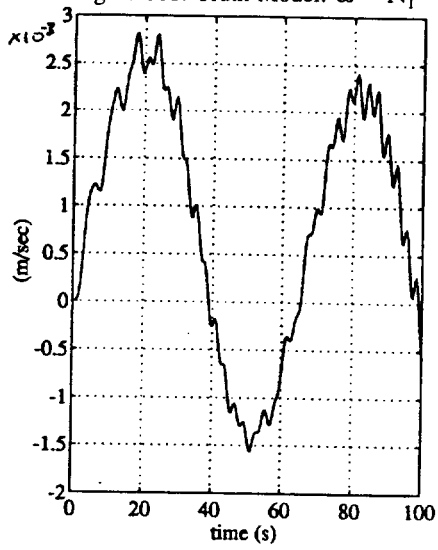

Figure 11a: Truth Model: $\mathbf{v}^{A^*} \cdot \mathbf{N}_1$

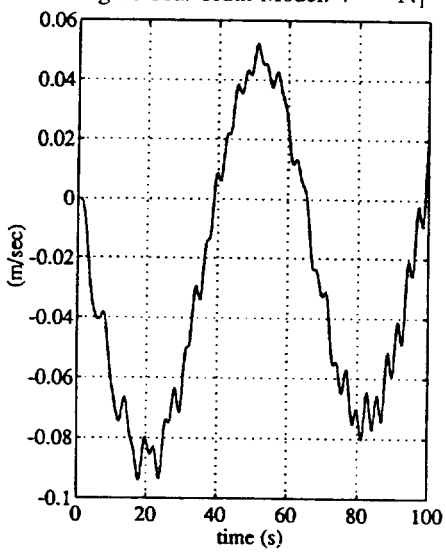

Figure 11b: Truth Model: $\mathbf{v}^{B^*} \cdot \mathbf{N}_1$

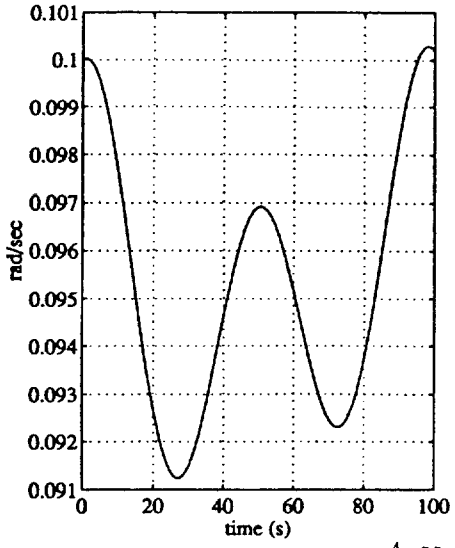

Figure 12a: Decoupled Method: $\omega^A \cdot \mathbf{N}_1$

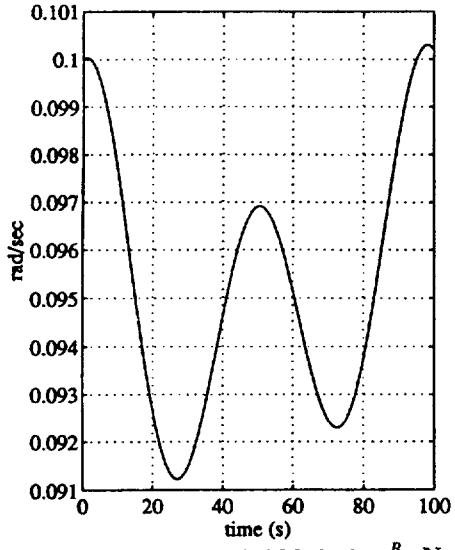

Figure 12b: Decoupled Method: $\omega^B \cdot \mathbf{N}_1$

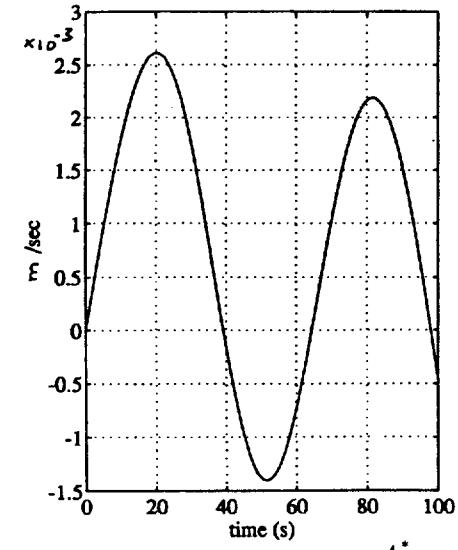

Figure 13a: Decoupled Method: $\mathbf{v}^{A^*} \cdot \mathbf{N}_1$

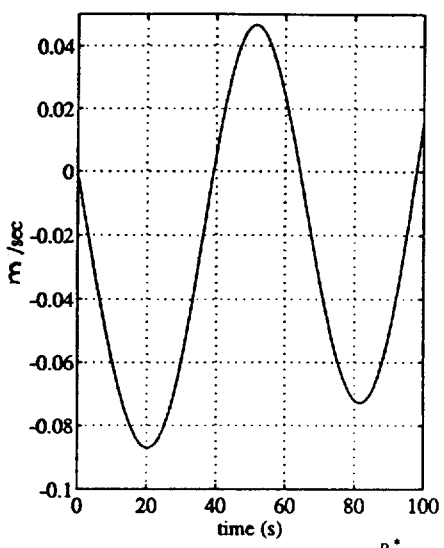

Figure 13b: Decoupled Method: $\mathbf{v}^{B^*} \cdot \mathbf{N}_1$

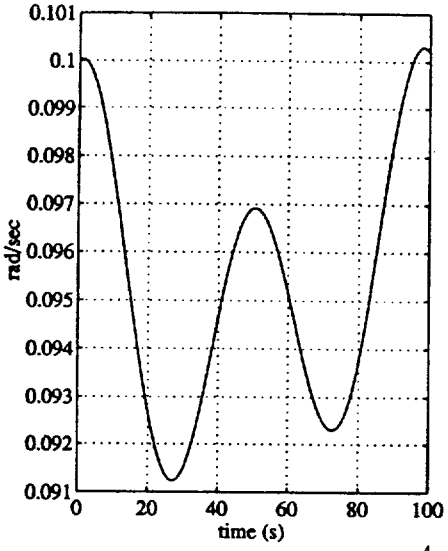

Figure 14a: One-Way-Coupled Model: $\omega^A \cdot \mathbf{N}_1$

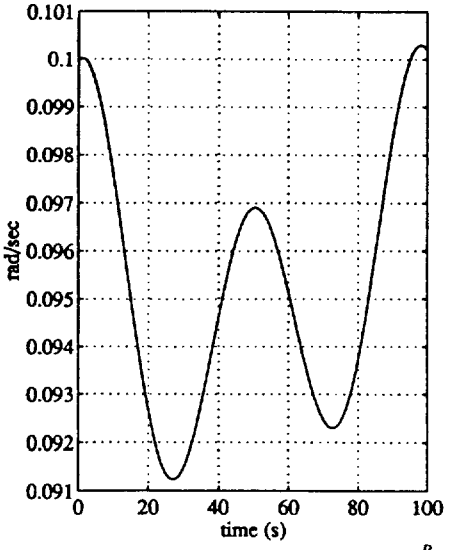

Figure 14b: One-Way-Coupled Model: $\omega^B \cdot \mathbf{N}_1$

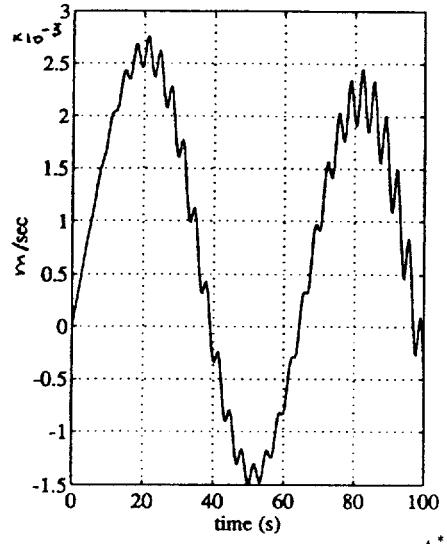

Figure 15a: One-Way-Coupled Model: $\mathbf{v}^{A^*} \cdot \mathbf{N}_1$

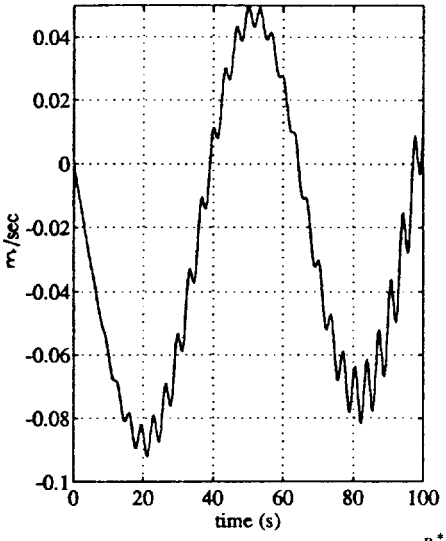

Figure 15b: One-Way-Coupled Model: $\mathbf{v}^{B^*} \cdot \mathbf{N}_1$